



Factors affecting strength of dissimilar TiAl/Ni–Si–B/Ni-based superalloy brazed joint

D. Kokabi¹ , A. Kafrou^{1,*} , R. Gholamipour¹ , and M. Pouranvari²

¹Department of Advanced Materials and Renewable Energies, Iranian Research Organization for Science and Technology, Tehran, Iran

²Department of Materials Science and Engineering, Sharif University of Technology, Tehran, Iran

Received: 15 November 2021

Accepted: 25 January 2022

Published online:
14 February 2022

© The Author(s), under exclusive licence to Springer Science+Business Media, LLC, part of Springer Nature 2022

ABSTRACT

This paper addresses the process-microstructure-strength correlation during dissimilar brazing of TiAl alloy to IN738 Ni-based superalloy using Ni–4Si–3.2B filler metal. The solid/liquid reactions, solidification phenomena, and solid-state phenomena are analyzed. The thickness of the athermal solidification zone and reaction layer at different bonding conditions (holding times and temperatures) determined and analyzed using a Larson–Miller parameter (LMP). It was resulted that the shear strength of the joint can be formulated regarding bonding temperature and holding time through using LMP. It was found that the sizes of athermally solidified zone and reaction layer are two key factors controlling the joint strength. The shear strength of the joints made at lower brazing temperature/times (i.e., low LMP) is controlled by the width of hard centerline eutectic borides. However, the width of the reaction layer is the dominating factor for the strength of the joints made at higher temperatures/times (i.e., high LMP). In addition, the highest shear strength of the joint was obtained in the optimum value of LMP.

Introduction

One of the fascinating alloys in recent years researches is the TiAl alloy. They are the most promising alternative to the prevalent heat-resistant steels and superalloys, especially in high-temperature applications [1, 2]. There are several possible applications of TiAl-based alloys in the aerospace, automotive, and

turbomachinery industries due to their good features, such as low specific gravity, high specific strength, good stiffness, good high-temperature mechanical properties, and oxidation resistance [3, 4].

Since it is not realistic to fabricate the entire set of assembly from TiAl alloys, the joining of TiAl to metallic materials has posed a significant challenge to the application of this alloy in the industry. Due to its simplicity and its low tolerance to surface condition,

Handling Editor: P. Nash.

Address correspondence to E-mail: ali.kafrou@irost.ir

<https://doi.org/10.1007/s10853-022-06971-w>

brazing is a preferred technique for joining difficult to weld TiAl/Ni-base superalloy combination.

One of the main parameters which indicates the microstructure and has great influence on the mechanical response of the bonded materials with the brazing method is the brazing filler alloy. There are intensive researches on the filler alloy selection for the brazing of TiAl alloys similar and dissimilar joining. Two kinds of alloys based on Ti and Ag are the most investigated as filler metals [5–8]. Guedes et al. [9] investigated microstructure and the chemical composition of the interfaces of the similar Ti–47Al–2Cr–2Nb joining using a Ti–15Ni–15Cu as braze alloy. Ni containing filler metals are one of the categories that has been studied as the potential filler for dissimilar TiAl/Ni-based superalloy joint. The first reason is the comprehensive researches on Ni-based superalloy joining by using Ni-based fillers [10, 11]. The second is the high tendency of Ti, Ni, and Al elements to form different compounds. Dong et al. [12] used a quinary FeCoNiSiB filler to vacuum braze TiAl/Ni-based superalloy. Tetsui [13] applied brazing of TiAl/Ni–Fe-based alloy with a Ni–Cr–B (BNi-9) as filler. He et al. [14] studied properties of Ti₃Al similar joint using NiCrSiB filler alloy. In our previous studies, TiAl was bonded with two different Ni-based filler alloys [15], and the TiAl/Ni-based superalloy was fabricated with a quinary NiCrFeSiB filler alloy [16].

According to previous studies on dissimilar bonding of TiAl to Ni-based superalloy using Boron-containing Ni-based filler alloys, it can be found that a specific joint region microstructure with different zones can be considered as the typical joint region microstructure. Thus, in the next paragraphs this typical microstructure will be explained.

Figure 1 shows schematic microstructure of the γ -TiAl/Ni–B/Ni-based superalloy brazed joint indicating the presence of three distinct zones in the bonding affected zone including (i) diffusion zone (DZ) in the Ni-based superalloy side, (ii) Reaction layer (RL) adjacent to the TiAl, and (iii) Solidification zone which is consisted of isothermal and athermal regions. The microstructure of the diffusion zone is influenced by diffusion of boron from the liquid into the Ni-based superalloy during the bonding process. Due to low solubility of B in Ni-based superalloys,

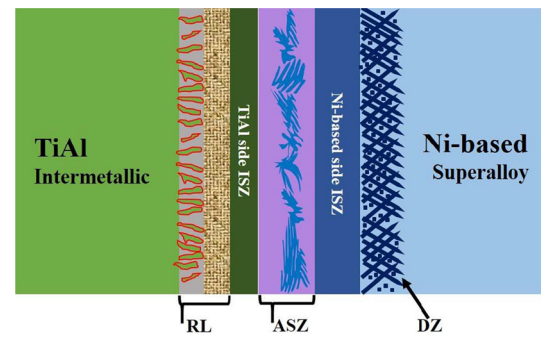


Figure 1 The schematic microstructure of a dissimilar TiAl/Ni-based superalloy brazed joint using a B-bearing Ni-based filler metal. ASZ, ISZ, DZ, and RL stand for: athermal solidification zone, isothermal solidification zone, diffusion zone, and reaction layer.

in situ precipitation of borides in the substrate region occurs [17].

In the reaction layer, due to the dissolution of the TiAl alloying elements into the molten filler metal, they react with Ni and lead to produce multiple layers consisted of Ti–Al–Ni intermetallic compounds [12, 14, 16]. The isothermal solidified zone in the Ni-based superalloy side is formed due to boron diffusion and raising the liquid temperature leading to solidification during holding at the bonding temperature. The microstructure of this zone is free from boron-containing intermetallics and consists of a solid solution phase. The TiAl side isothermal solidified zone consisted of the solid solutions due to the intense dissolution of TiAl alloying element into the molten filler [16]. In the final stage of the joint formation, if the liquid remains at the end of the bonding time, it will be solidified upon cooling usually via binary/ternary eutectic reactions that lead to the formation of a network of hard boride phases.

Considering the presence of various microstructural zones in the brazing affected zone of dissimilar TiAl/Ni-base superalloy combination, the question is what is the role of each microstructural zone on the joint strength. Therefore, this work highlights the microstructure-property relationships during dissimilar brazing of γ -TiAl to Inconel 738 Ni-based superalloys using a boron-containing filler metal. The key factors controlling the joint strength are discussed.

Materials and methods

Materials

Titanium and aluminum with high purity (99.97 and 99.7 wt.%, respectively) were used for producing TiAl intermetallic compound. Alloying and casting in $2 \times 10 \times 30$ mm mold were carried out in a Vacuum Arc Remelting (VAR) furnace. A cast IN738 (Ni–16.3Cr–1.9Nb–1.75Mo–3.4Ti–3.2Al–8.5Co–0.3Si–2.6W–0.17C in wt.%) was used as the other base metal. A commercial amorphous foil Ni–4Si–3.2B (wt.%) alloy (BNi-3) with a thickness of 50 microns was used as the filler metal.

Brazing procedure

Figure 2b shows a schematic of the bonding set-up. The size of the samples was $2 \times 10 \times 10$ mm. The gap size was set as 50 μm . In fact, the thickness of Ni-based filler alloy is 50 μm which is inserted between the two substrates. The bonding experiments were conducted at the temperature range of 1100–1175 $^{\circ}\text{C}$ for 5–60 min according to the design of experiments which have been shown in Table 1. During all of the bonding experiments, the vacuum was kept at 6×10^{-3} Pa with using rotary and diffusion vacuum pumps. The heating rate in all of bonding was 10 $^{\circ}\text{C}/\text{min}$ and cooling after finishing the bonding was 15 $^{\circ}\text{C}/\text{min}$ with maintaining the vacuum condition in the furnace until reaching the 600 $^{\circ}\text{C}$, then samples air cooled to the room temperature. Bonding temperatures and their relevant holding times at bonding temperature are written in Table 1.

After bonding, samples placed in the designed fixture for evaluating their shear strength. The shear strengths for the brazed joints were measured at

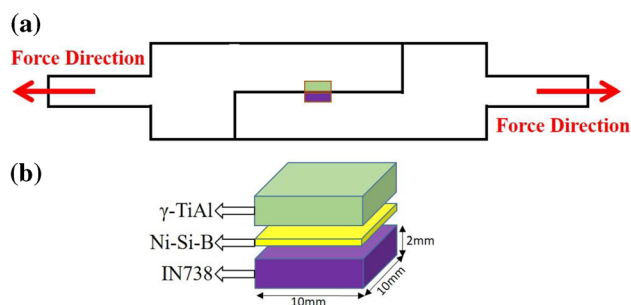


Figure 2 a The schematic setup of the fixture used for the shear test, b the schematic sandwiched sample which brazed and then placed in the shear test fixture.

room temperature using a fixture (Fig. 2a) employing a testing machine (SANTAM 250). The reported average strength was obtained from at least three joint specimens. The fracture surfaces were studied by X-ray diffraction (PANalytical X'Pert Pro MPD) for phase analysis. The microstructures of the joints and semi-quantitative chemical analysis of phases formed in the joint region were examined using optical microscopy (Olympus BX-60) and field-emission scanning electron microscope FEI ESEM Quanta 200, equipped with EDAX EDS Silicon Drift 2017 and a scanning electron microscope (SEM, JEOL JXA-840) for imaging. The Micro-hardness test of the typical microzones across the TiAl/IN738 joints was performed using a Vickers hardness tester with a load of 30 g and load time of 10 s.

Results

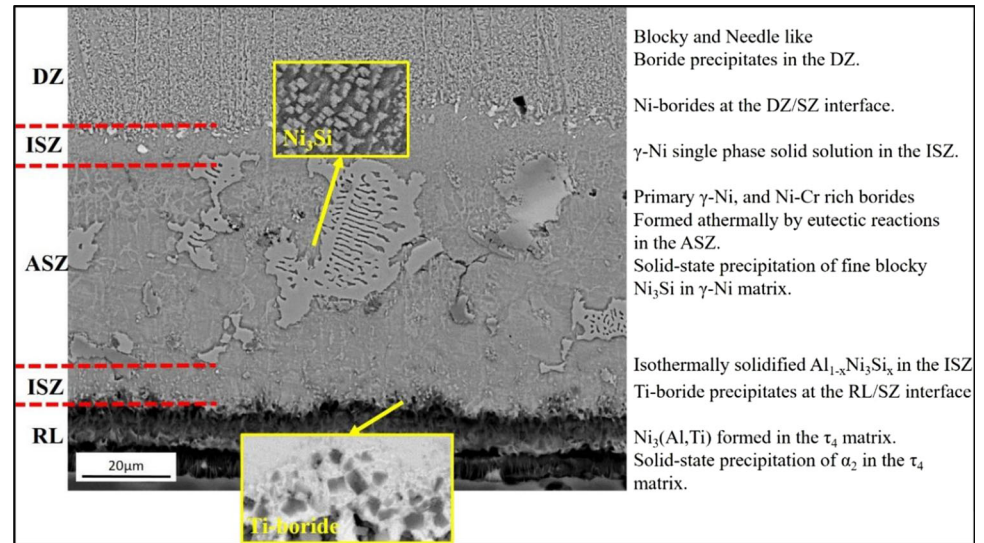
Microstructure evaluation of the TiAl/IN738 joint

Figure 3 shows the typical microstructure of the TiAl/Ni–Si–B/IN738 brazed joint made at 1150 $^{\circ}\text{C}/5$ min indicating formation of DZ, ISZ, ASZ and RL in the brazing affected zone. The different phases and zones which have been formed within the brazed joint will be completely analyzed and explained. The main feature for this brazed joint is its thick athermally solidified central zone that regarding its continuous brittle nature [10] can cause lower strength and more brittle behavior in comparison with other brazed joints which bonded at higher bonding holding times. It can lead to have the joint with thinner ASZ or even with no athermally solidified region in the solidified zone. Table 2 shows FESEM-EDS composition analysis of the phases formed in various microstructural zones according to Fig. 4. The key microstructural features of the TiAl/Ni–Si–B/IN738 brazed joints are summarized, as follows:

- (i) Solidification zones:
An isothermal solidified continuous solid solution between the two isostructural binary $\text{Al}_{1-x}\text{Ni}_3\text{Si}_x$ in the TiAl side [16]. On the other side, the solidification of the γ -Ni solid solution in the two ways, isothermally during holding time at the bonding temperature in the ISZ and athermally during the cooling

Table 1 Schedule of bondings

Bonding temperature (°C)	1100	1120	1120	1150	1150	1150	1175
Holding time (min)	20	20	60	5	20	45	20

Figure 3 The typical microstructure of the TiAl/Ni–Si–B/IN738 brazed joint made at 1150 °C/5 min.**Table 2** The FESEM-EDS chemical composition (at. %) of phases formed (see Fig. 4) in different microstructural zones of the TiAl/Ni–Si–B/IN738 brazed joint

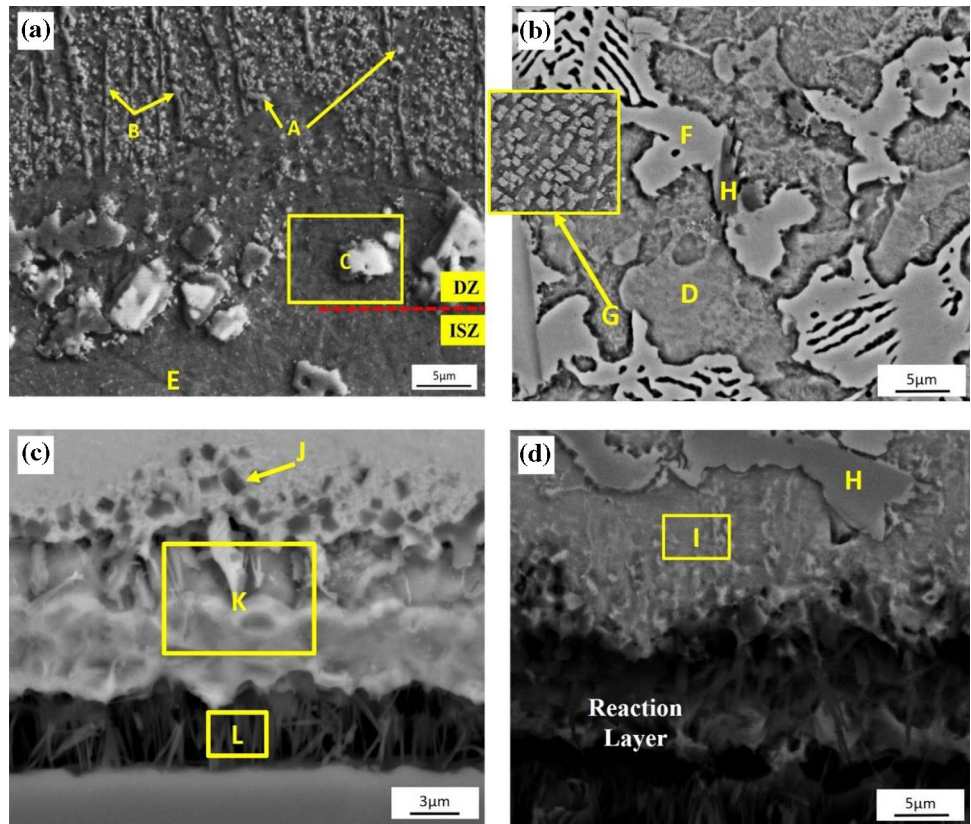
Zone	Possible Micro-constituents	Elements								
		Ni	Cr	Co	Si	Mo	Ti	Al	Nb	W
DZ	A Blocky precipitate ^a	57.3	19.8	2.4	0.5	8.4	3.5	2.1	1.8	4.2
	B Needle-like precipitate ^a	60.3	18.2	1.4	0.4	10.2	2.2	1.9	2.2	3.2
	C Ni-boride ^a + γ -Ni	84.2	4.3	1.9	0.5	0.4	3.2	3.3	0.9	1.3
SZ	D γ -Ni	66.9	11.2	6.6	1.2	1.2	3.6	6.5	1.2	1.6
	E Primary γ -Ni	78.9	2.2	5.4	0.9	4.9	3.2	2.4	0.9	1.2
	F Ni-boride ^a	88.5	1.9	1.8	–	1.7	1.5	1.2	1.5	1.9
	G Eutectic γ + Ni_3Si	74.5	2.8	6.3	15.1	0.3	0.5	0.3	–	0.2
	H Cr-boride ^a	2.1	81.4	0.7	–	8.8	1.2	2.2	1.4	2.2
	I $\text{Al}_{1-x}\text{Ni}_3\text{Si}_x$	71.2	1.7	1.5	8.5	0.8	1.6	14.7	–	–
	J Ti-boride ^a	9.2	2.7	1.5	–	–	82.1	4.2	–	0.3
RL	K τ_4 -TiNi ₂ Al + $\text{Ni}_3(\text{Al},\text{Ti})$	72.6	0.6	1.7	0.7	–	12.4	11.8	–	0.2
	L τ_4 -TiNi ₂ Al + α_2 -Ti ₃ Al	36.6	0.3	0.6	0.2	–	37.5	24.6	–	0.2

^a Boron could be detected by the EDS in this phase, though it could not be quantified due to the inability of the EDS system for the light elements

stage within the ASZ [11, 18]. ISZ of IN738 side composed of a thin layer of γ nickel base solid solution which is created at the solid/liquid interface due to the isothermal solidification at the bond temperature. By increasing the holding time at the bonding temperature, the higher portion of the middle solidified zone will be solidified during isothermal process. The boride phase formations during on-cooling solidification occur

due to segregation of B as a product of the binary and/or ternary eutectics in the center of the SZ [11, 18]. The formation of boride phase is accompanied by Si rejection due to the insolubility of Si in boride [18]. Therefore, during cooling from bonding temperature, the excess amount of Si should be rejected from γ solid solution as some fine blocky β_1 - Ni_3Si particles by a solid-state precipitation reaction.

Figure 4 Different zones microstructures of the TiAl/Ni–Si–B/IN738 brazed joint made at 1150 °C/5 min, **a** borides phases at DZ and Ni-solution at ISZ, **b** phases at Solidified Zone, **c** phases at SZ near the TiAl substrate, **d** different phases at Reaction Layer.



(ii) Reaction layer:

The reaction layer (RL) of the joint consisted of multiple regions. The lamellar phase that discontinuously distributed at the RL/TiAl substrate is the α_2 -Ti₃Al [19]. The formation of this phase relates to the interdiffusion between the TiAl base material and the solidified bond region. Considering the morphology of the Ti₃Al, this phase has resulted from a solid-state diffusion [20]. Due to the consumption of Ti and Al during the formation of the α_2 phase, the concentration of the Ni will increase and the matrix of this phase at the RL adjacent to the TiAl can be the τ_4 -TiNi₂Al. The other part of the reaction layer is mainly composed of the τ_4 -TiNi₂Al phase containing γ' -Ni₃(Al, Ti) precipitates. At the RL/SZ interface of the joint some fine blocky precipitates have been formed. They are enriched with Ti, and the boron peak indicated at the EDS spectrum that can be referred to as the Ti-boride phase [14]. Due to the formation of the Ti-borides at a temperature higher than the bonding

temperature, it can be concluded that these Ti-borides precipitated as solid-state precipitation.

(iii) Diffusion zone:

Due to boron diffusion into the IN738, some borides precipitated in the solid substrate and formed a distinct zone named DZ. The enrichment of precipitates with Cr and Mo shows that they can be considered as Cr–Mo rich borides, and according to their morphology (blocky and needle-like), they have been formed during the holding time at the bonding temperature [18]. On the other hand, some discontinuous nickel rich borides have been formed during the heating stage due to boron diffusion to the initial liquid/solid interface and the presence of Ni at the interface [21, 22].

In general, the common phase sequence within the TiAl/Ni–Si–B/IN738 joint from the TiAl side to the IN738 can be described as follows: TiAl substrate/ α_2 -Ti₃Al + τ_4 -TiNi₂Al/ τ_4 -TiNi₂Al + γ' -Ni₃(Al, Ti)/Al_{1-x}Ni₃Si_x + Ti-boride/ γ -Ni + Cr–Ni-rich borides/ γ -Ni/Cr–Mo borides/IN738 substrate.

Figure 5 shows the typical hardness profile of the brazed joint. Generally, it can be seen that the hardness distribution is nonuniform due to severe microstructure gradient, and the hardness of phases formed in the joint region is higher than the substrates. The centerline borides possess the maximum hardness in the whole bonded area, and the hardness of the RL and DZ is lower than that of ASZ borides. The important point is to evaluate how the mechanical properties are affected by this microstructure gradient.

Mechanical properties of the TiAl/IN738 joint

Figure 6 shows the room-temperature shear strength of the joints. As can be seen, the brazing conditions significantly affect the joint strength. The highest and the lowest shear strength were achieved in the joints made at 1120 °C/60 min and 1100 °C/20 min, respectively.

As it is discussed in the next sections, the joint strength is controlled by the size of the reaction layer and ISZ. Since, the growth of these layers during brazing is diffusion controlled, the sizes of reaction layer and ISZ brazing temperature and time. Therefore, brazing time and temperature affect the mechanical strength. According to previous studies [23, 24], a combined parameter in the form of Larson–Miller parameter, $T(C + \text{Log}t)$ can be used to correlate the joint strength to the brazing parameters. Figure 7 shows the effect of a Larson–Miller parameter ($T(20 + \text{Log}t)$) on the shear strength of TiAl/Ni–

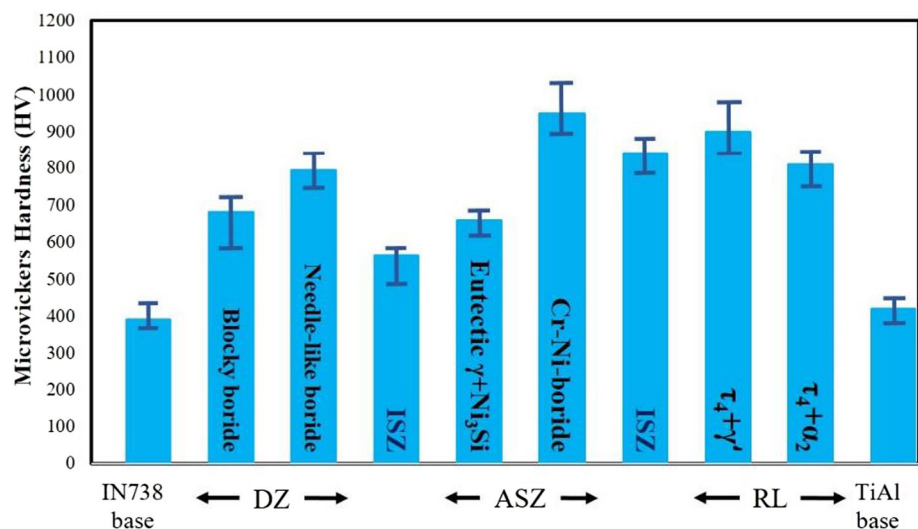
Si-B/IN738. The plot can be divided into three zones. The highest joint strength levels were obtained Zone II, and the lowest strength levels were obtained in Zone I.

Parameters affecting the microstructure

Table 3 shows the effect of bonding conditions on the joint strength and the size of critical microstructural zones (i.e., ASZ and RL in the TiAl side). Figure 8 shows the effect of LMP on the size of ASZ and RL. The ASZ size is controlled by the progress of the diffusion-induced isothermal solidification, which is governed by bonding temperature and the bonding time. Increasing bonding temperature and bonding time (i.e., increasing the LMP) enhanced the diffusion of boron in the base metals, resulting in reducing the ASZ size. However, when bonding at 1175 °C, the ASZ was thickened, which indicates a reduction in isothermal solidification rate at this bonding temperature. It is reported in the previous works on TLP bonding of precipitation-hardened nickel-based superalloys (e.g., IN738 and GTD-111) that there is a critical bonding temperature which beyond that the rate of isothermal solidification reduces due to the enrichment of residual liquid with some BM alloying element, particularly Ti during dissolution and isothermal solidification stages [25, 26].

According to Fig. 8, the size of RL is increased by increasing LMP. The size of the RL in TiAl side is controlled by the reaction of nickel and TiAl which is diffusion-controlled process. Therefore, bonding using a longer holding time or a higher bonding

Figure 5 Hardness distribution in the TiAl/Ni–Si–B/IN738 joint at 1150 °C for 5 min.



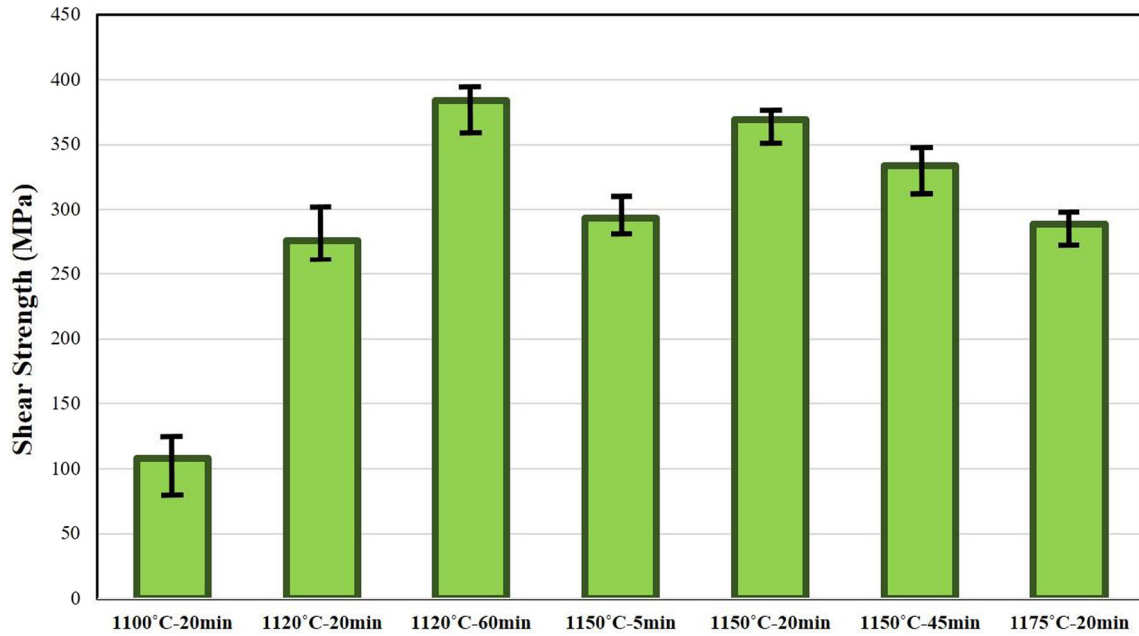


Figure 6 Shear strength of the TiAl/Ni–Si–B/ IN738 brazed joints.

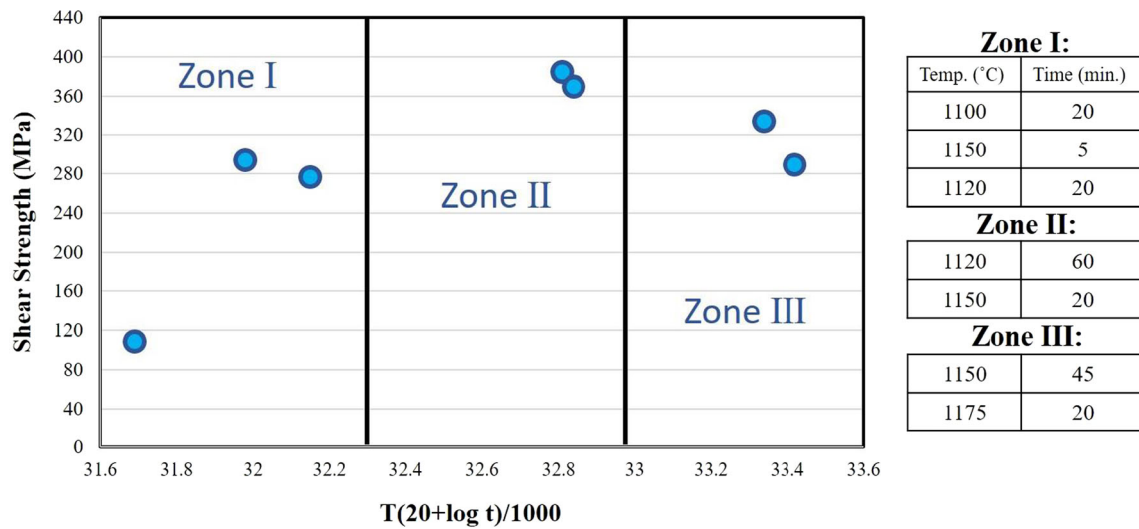


Figure 7 Shear strength versus Larson–Miller parameter of the TiAl/Ni–Si–B/IN738 brazed joints.

Table 3 The relation between Larson–Miller parameter of the brazing process and width of the zones within the brazed joints

Zone	T (°C)	T (min)	T(20 + Logt)/1000	Shear strength (MPa)	ASZ size (µm)	RL size (µm)
I	1100	20	31.688	108	56.2	14.2
I	1120	20	32.149	276	46.5	19.5
II	1120	60	32.814	384	19.5	26.1
I	1150	5	31.985	294	40.5	17
II	1150	20	32.842	369	17	32.5
III	1150	45	33.343	334	14.6	40.8
III	1175	20	33.419	289	39.2	38.3

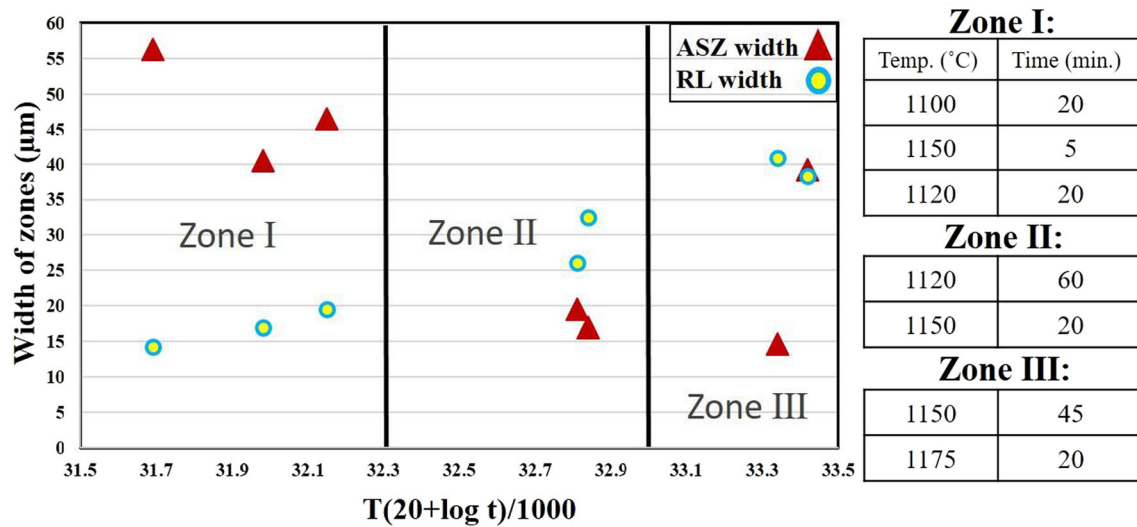


Figure 8 Width of the ASZ and the RL zones versus Larson-Miller parameter of the TiAl/Ni–Si–B/IN738 brazed joints.

temperature resulted in the wider RL that could adversely affect the joint's mechanical properties [14].

Discussion

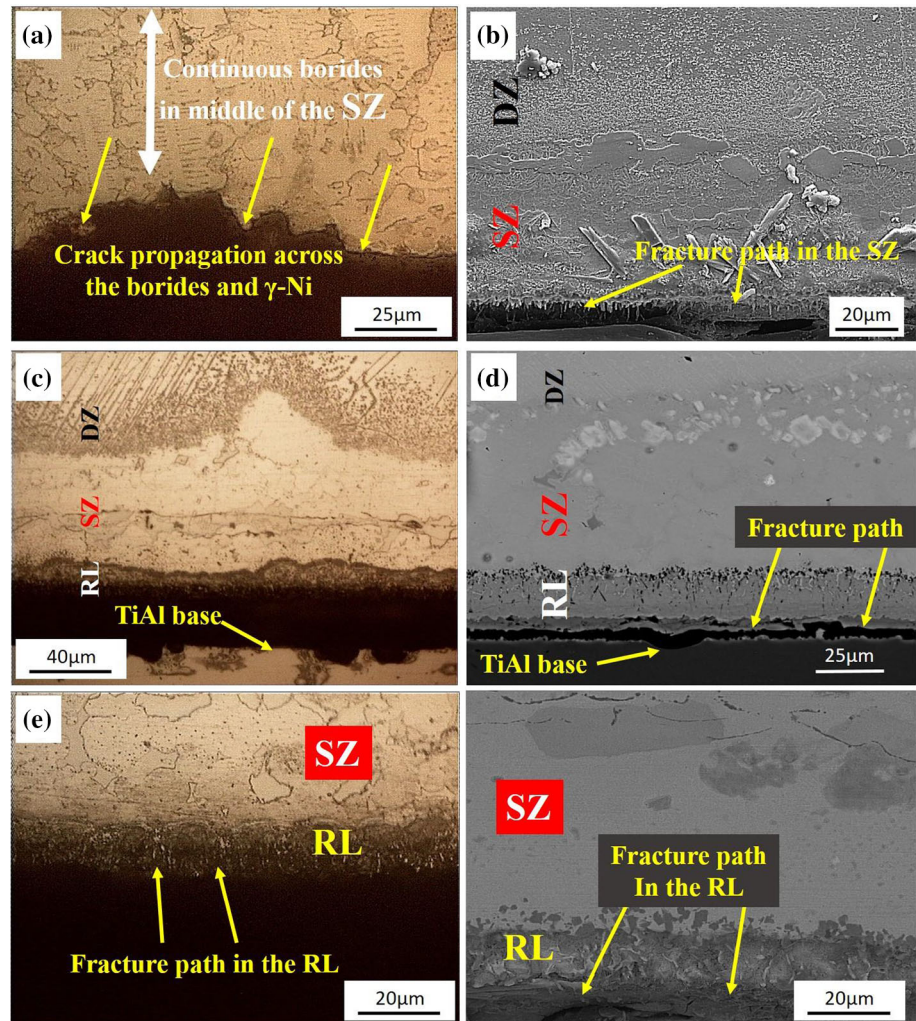
Failure path analysis

Three fractured joints were studied as representing three different zones (introduced in Fig. 7) using an optical microscope and X-ray diffraction. Figure 9 shows the metallographic and SEM images cross section of the fracture path. Figure 10 shows the XRD patterns of the fracture surface of the samples after shear testing. According to Fig. 9a–b, the fracture of the joint made at 1100 °C/20 min (Zone I) occurred through ASZ due to the presence of a continuous network of hard and brittle boride phases. The presence of boride phases on the fracture surface of this sample is evident in XRD pattern (Fig. 10a). According to Fig. 9c–d, the fracture of the joint made at 1120 °C/60 min (Zone II) occurred via crack propagation partly through RL/TiAl interface and partly through TiAl base metal, as it is confirmed by the XRD patterns given in Fig. 10b. According to Fig. 9e–f, the fracture of the joint made at 1150 °C/45 min (Zone III) occurred via crack propagation through RL, as it is confirmed by the XRD pattern give in Fig. 10c.

LMP-strength correlation

According to preceding discussion, the size of boride containing eutectic-type structure of the ASZ and the size of IMC containing reaction layer at the TiAl side are two key parameters controlling the joint strength. Notably, the formation of boride phases in DAZ of IN738 does not seem to play an essential role in joint strength. The fine-scale and the discrete morphology of boride phases in DAZ explain why they did not provide a preferential path for the joint failure. The sizes of ASZ and RL are controlled by the combined effect of time and temperature of the brazing process. Therefore, the sizes of ASZ and RL can be correlated with brazing LMP value. Figure 11 shows the effect of brazing LMP on the joint microstructure. According to Fig. 11 the joint made at 1100 °C/20 min, a low LMP value brazing condition, consisted of a thick ASZ and a thin RL. The presence of a thick ASZ which contains a continuous network of hard and brittle boride phase provide an easy crack propagation path. Therefore, the presence of a thick ASZ is potential source for failure of TiAl/Ni–Si–B/IN738 brazed joint. It can be concluded that the strength of the joints in Zone I (brazing using low LMP value) is controlled by the size of the athermal solidification zone. Therefore, to enhance the joint strength the size of the ASZ should be reduced via allowing more liquid to be solidified isothermally. Therefore, increasing LMP value can enhance the joint strength via decreasing ASZ size of the properties. Figure 11b shows microstructure of the joint made at 1100 °C/

Figure 9 Optical and SEM micrographs of failure path in the TiAl/Ni–Si–B/IN738 brazed joints: **a–b** joint at 1100 °C for 20 min, the fracture propagates across the continuous athermally solidified eutectic microstructure, **c–d** joint at 1120 °C for 60 min, the failure occurred in the TiAl base and the RL/TiAl interface, and **e–f** joint at 1150 °C for 45 min, the thick RL is responsible for the major part of the fracture.

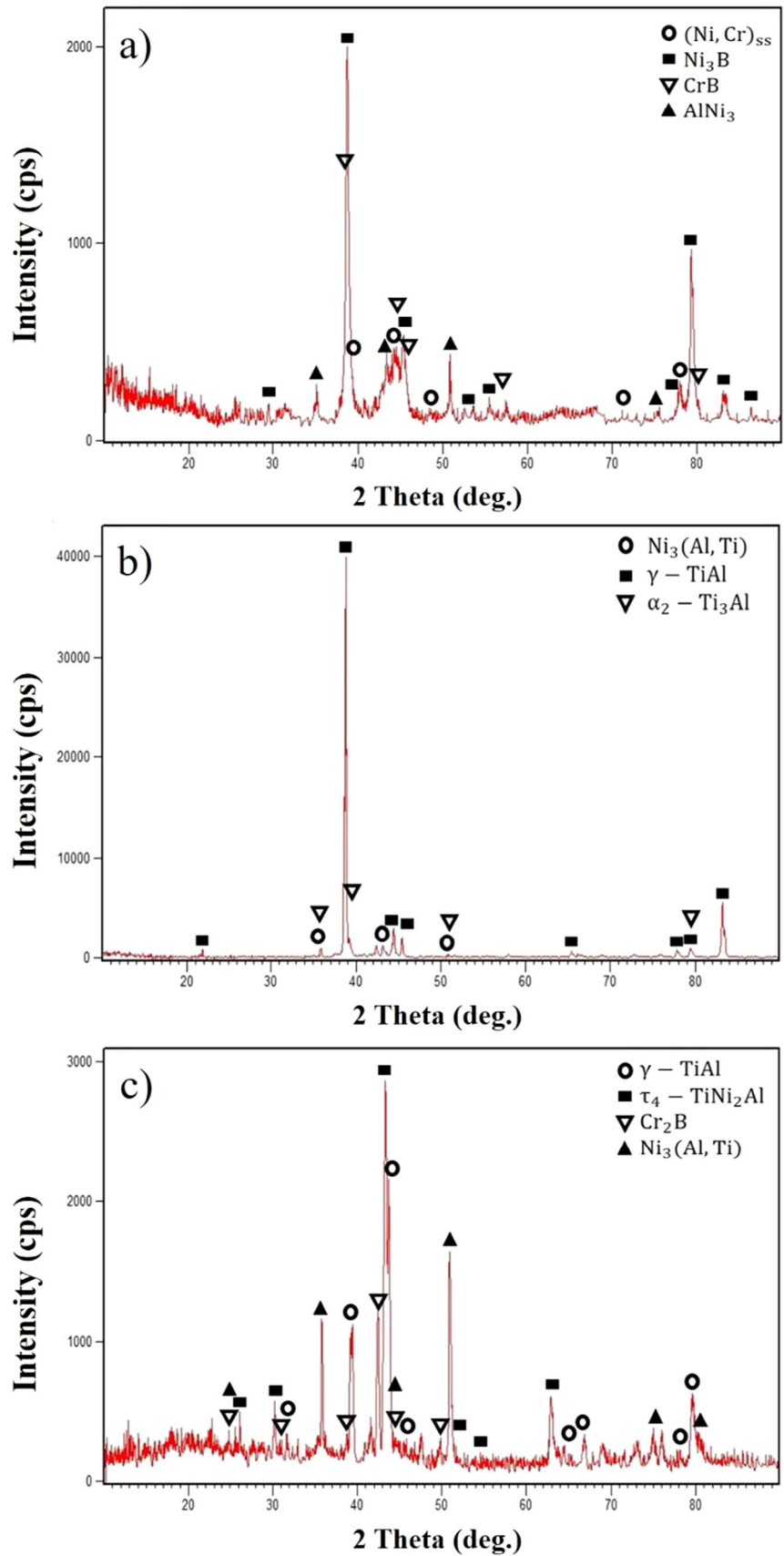


60 min, a medium LMP value brazing condition, indicating a significant reduction in ASZ size. Despite further increasing the LMP value of the brazing condition (brazing in Zone III) can decrease the ASZ size, the joint strength was decreased, beyond a critical value. As evidenced by the fracture path and XRD pattern of the fracture surface, the strength of the joints made a high LMP values is controlled by the brittleness of the reaction layer. The size of RL is controlled by the diffusion. Therefore, as shown in Fig. 11c, the microstructure of the joint made at 1150 °C/45 min, a high LMP value brazing condition, consisted of a thin ASZ but thick RL. The thickness of the RL in joint made at 1150 °C/45 min is 40.8 μm which is significantly higher than that of joint made at 1120 °C/20 min (i.e., 14.2 μm). This can explain why joint strength is decreases in high value LMP brazing conditions.

Table 4 provides a comparison of achieved strength in dissimilar brazing between TiAl-based alloy and Ni-based superalloys using various filler metals or joining methods. Considering the fact that generally shear strength is lower than the tensile strength, according to Table 4 it can be seen that the achieved shear strength in this study is higher compared to the shear strength of other works. Therefore, it can be concluded that brazing using Ni–Si–B filler metal is a good choice for brazing of TiAl/Ni-based superalloy due to its considerable shear strength compared to the other studies. The maximum achievable strength in TiAl/Ni–Si–B/IN738 is rely on the controlling the size of the ASZ and also the RL in TiAl side which in turn requires precise optimization of bonding temperature and bonding time.

The main phases which identified on the fractured surfaces of the previous studies and current study also have been written in Table 4. The interesting

Figure 10 XRD patterns of the fractured surfaces of the TiAl/Ni–Si–B/IN738 brazed joints made at: **a** 1100 °C for 20 min declares the presence of the boride phases in the fractured surface due to the fracture occurring at the SZ, **b** 1120 °C for 60 min, it can be seen that γ -TiAl is the major phase present in the fractured surface, and **c** 1150 °C for 45 min shows that the τ_4 and γ' are the major phases present in the fractured surface.



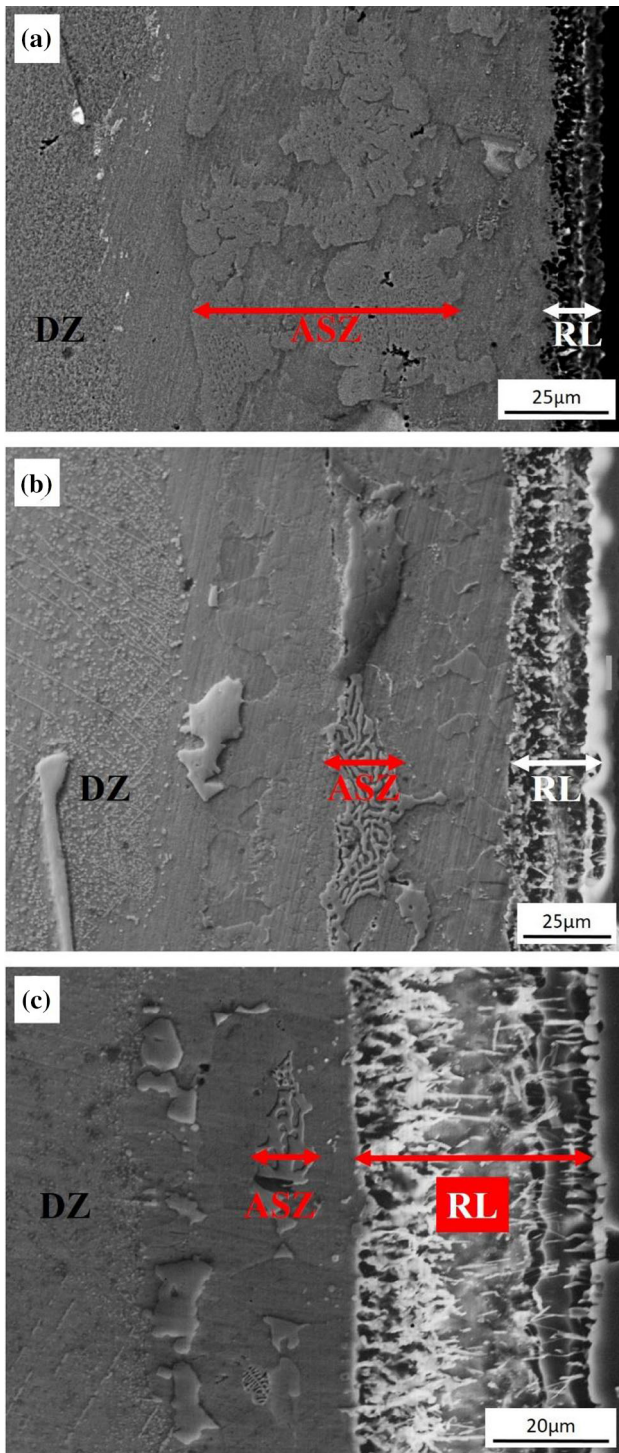


Figure 11 SEM micrographs of the TiAl/Ni-Si-B/IN738 brazed joints of three LMP different zones: **a** Zone I, at 1100 °C for 20 min, **b** Zone II, at 1120 °C for 60 min., and **c** Zone III, at 1150 °C for 45 min.

point which can be derived from all of the fractured surfaces is that the fracture has occurred in the joint region near to the TiAl side. In other words, the major phases in the fractured surfaces are related to the microstructures which are formed during solid/liquid reactions in the TiAl-base side. In our study, the main phases identified in the fractured surface are α_2 -Ti₃Al and the TiAl substrate which shows that the strength of the joint region is comparably high that lead to change the fracture path through the TiAl substrate.

Conclusions

The key microstructural features of the IN738/Ni-Si-B/TiAl brazed joints are (i) boride phase formation in the joint centerline during on-cooling solidification due to the strong segregation of B, (ii) in-situ solid-state precipitation of Cr-Mo rich boride in the diffusion zone of the IN738 substrate, and (iii) formation of various intermetallic phases (e.g., Ti-Ni-Al intermetallic compounds) in the reaction layer between TiAl and liquid filler metal. It is found that the size of boride containing eutectic-type which was formed during athermal solidification of the remaining liquid in the joint gap and thickness of Ti-Ni-Al the intermetallic containing which was formed as a result of the reaction between liquid filler metal and TiAl base metal are two key controlling factor of the joint strength. It is found that the formation of a thick and continuous network of boride phases in athermal solidification zone in the joints made using low LMP value brazing conditions can provide a low fracture toughness easy crack growth path which limits the achievable strength. Enhanced joint strength can be obtained by increasing the LMP value of the brazing conditions via decreasing the size of the ASZ. However, brazing at high LMP value conditions has an adverse effect on the join strength due to formation a thick reaction layer.

Table 4 Comparison of dissimilar TiAl/Ni-based superalloy joints with different filler metals

Reference	Substrate/Filler	Brittle phases on fractured surface	Strength(MPa)	Joining method
Dong et al. [27]	TiAl/Zr–Al–Ni–Co/Ni alloy	Intermediate zone	353 (shear)	Brazing
Ren et al. [28]	Ti ₃ Al/Au–Ni/Ni alloy	τ_4 -TiNi ₂ Al	434 (tensile)	Brazing
Cai et al. [29]	TiAl/V/Cu/Ni alloy	γ -TiAl, α_2 -Ti ₃ Al	230 (tensile)	Laser Weld
Ren et al. [8]	Ti ₃ Al/Ag–Cu–Pd/Ni alloy	Ni ₃ Ti, Ti ₃ Pd ₅	404 (tensile)	Brazing
Dong et al. [12]	TiAl/Fe–Co–Ni–Si–B/Ni alloy	γ -TiAl, α' -Fe(Co Ni)	363 (shear)	Brazing
Dong et al. [30]	TiAl/Zr–Al–Ni–Cu/Ni alloy	γ -TiAl	415 (tensile)	ThermoPlastic Bonding
This study	TiAl/Ni–Si–B/Ni alloy	γ -TiAl, α_2 -Ti ₃ Al	384 (shear)	Brazing

Acknowledgements

This research was done in EnerMat laboratory at Iranian Research Organization for Science and Technology (IROST) under grant number 1012095010. The authors would like to acknowledge the IROST for funding this research.

References

- Dimiduk DM, Miracle DB, Ward CH (1992) development of intermetallic materials for aerospace systems. *Mater Sci Technol* 8:367–375
- Noda T (1998) Application of cast gamma TiAl for automobiles. *Intermetallics* 6:709–713
- Yamaguchi M, Inui H, Kazuhiro I (2000) High-Temperature Structural Intermetallics. *Acta Mater* 48:307–322. [https://doi.org/10.1016/S1359-6454\(99\)00301-8](https://doi.org/10.1016/S1359-6454(99)00301-8)
- Kim YW (1994) Ordered intermetallic alloys, Part III: Gamma titanium aluminides. *JOM* 46(7):30–39. <https://doi.org/10.1007/BF03220745>
- Shiue RK, Wu SK, Chen SY (2003) Infrared brazing of TiAl intermetallic using BAg-8 braze alloy. *Acta Mater* 51:1991–2004
- Song XG, Cao J, Chen HY, Wang YF, Feng JC (2012) Brazing TiAl intermetallics using TiNi–V eutectic brazing alloy. *Mater Sci Eng A* 551:133–139
- Shiue RK, Wu SK, Chen YT, Shiue CY (2008) Infrared brazing of Ti50Al50 and Ti–6Al–4V using two Ti-based filler metals. *Intermetallics* 16(9):1083–1089
- Ren HS, Xiong HP, Long WM, Shen YX, Pang SJ, Chen B, Cheng YY (2018) Interfacial diffusion reactions and mechanical properties of Ti₃Al/Ni-based superalloy joints brazed with AgCuPd filler metal. *Mater Characterization* 144:316–324
- Guedes A, Pinto AMP, Vieira MF, Viana F (2003) Joining Ti-47Al-2Cr-2Nb with a Ti/(Cu,Ni)/Ti clad-laminated braze alloy. *J Mater Sci* 38:2409–2414. <https://doi.org/10.1023/A:1023948917115>
- Pouranvari M, Ekrami A, Kokabi AH (2017) Microstructure evolution mechanism during post-bond heat treatment of transient liquid phase bonded wrought IN718 superalloy: an approach to fabricate boride-free joints. *J Alloys Compounds* 723:84–91
- Ghasemi A, Pouranvari M (2018) Microstructural evolution mechanism during brazing of Hastelloy X superalloy using Ni–Si–B filler metal. *Sci Technol Welding Join* 23:441–449
- Dong K, Kong J, Yang Y, Peng Y, Zhou Q, Wang K (2020) Achieving high-strength joining of TiAl- and Ni-based alloys at room temperature and 750°C via utilizing a quinary FeCoNi-based amorphous filler. *J Mater Res Technol* 9(2):1955–1965
- Tetsui T (2001) Effect of brazing filler on properties of brazed joints between TiAl and metallic materials. *Intermetallics* 9:253–260
- He P, Feng J, Zhou H (2004) Microstructure and strength of brazed joints of Ti₃Al-base alloy with NiCrSiB. *Mater Characterization* 52:309–318
- Kokabi D, Kafrou A (2020) Phase transformation study during diffusion brazing of γ -TiAl intermetallic using amorphous Ni-based filler metals. *Mater Sci Technol* 36(15):1639–1647
- D. Kokabi, A. Kafrou, M. Pouranvari, R. Gholamipour, Microstructural evaluation during dissimilar transient liquid phase bonding of TiAl/Ni-based superalloy. *J Alloys Compounds* 825 (2020) 153999.
- Sheng NC, Hu XB, Liu J, Jin T, Sun XF, Hu ZQ (2015) M3B2 and M5B3 Formation in diffusion-affected zone during transient liquid phase bonding single-crystal superalloys. *Metal Mater Trans A* 46A:1670–1677
- Pouranvari M, Ekrami A, Kokabi AH (2013) Solidification and solid state phenomena during TLP bonding of IN718 superalloy using Ni–Si–B ternary filler alloy. *J Alloys Compounds* 563:143–149

- [19] H. Li, H. Wei, P. He, T. Lin, J. Feng, Y. Huang, Effects of alloying elements in GH99 superalloy on microstructure evolution of reactive brazing TiAl/GH99 joints. *Intermetallics* 34 (2013) 69–74.
- [20] Ren HS, Xiong HP, Chen B, Pang SJ, Chen BQ, Ye L (2016) Microstructures and mechanical properties of vacuum brazed Ti3Al/TiAl joints using two Ti-based filler metals. *Mater Sci Technol* 32:372–380
- [21] Gale WF, Wallach ER (1991) Microstructural development in transient liquid-phase bonding. *Metal Mater Trans A* 22A:2451–2458
- [22] Gale WF, Guan Y (1999) Microstructure and mechanical properties of transient liquid phase bonds between NiAl and a Nickel-Base superalloy. *J Mater Sci* 34:1061–1071. <https://doi.org/10.1023/A:1004504330294>
- [23] Limarga AM, Iveland J, Gentleman M, Lipkin DM, Clarke DR (2011) The use of Larson-Miller parameters to monitor the evolution of Raman lines of tetragonal zirconia with high temperature aging. *Acta Mater* 59(3):1162–1167
- [24] Pouranvari M, Ekrami A, Kokabi AH (2013) TLP bonding of cast IN718 nickel based superalloy: Process–microstructure–strength characteristics. *Mater Sci Eng A* 568:76–82
- [25] Pouranvari M, Ekrami A, Kokabi AH (2009) Effect of bonding temperature on microstructure development during TLP bonding of a nickel base superalloy. *J Alloy Compd* 469(1):270–275
- [26] Idowu OA, Richards NL, Chaturvedi MC (2005) Effect of bonding temperature on isothermal solidification rate during transient liquid phase bonding of Inconel 738LC superalloy. *Mater Sci Eng A* 397:98–113
- [27] Dong K, Kong J (2019) A high-strength vacuum-brazed TiAl/Ni joint at room temperature and high temperature with an amorphous foil Zr-Al-Ni-Co filler metal. *J Manufact Process* 44:389–396
- [28] Ren HS, Xiong HP, Long WM, Chen B, Shen YX, Pang SJ (2019) Microstructures and mechanical properties of Ti3Al/Ni-based superalloy joints brazed with AuNi filler metal. *J Materials Science & Technology* 35:2070–2078
- [29] X. Cai, D.Q. Sun, H. Li, C. Meng, L. Wang, C. Shen, Dissimilar joining of TiAl alloy and Ni-based superalloy by laser welding technology using V/Cu composite interlayer. *Optics and Laser Technology* 111 (2019) 205–213.
- [30] K.W. Dong, J. Kong, Z.X. Wei, Y. Yang, Y.L. Liang, Y. Peng, Q. Zhou, K.H. Wang, Thermoplastic bonding (TPB) of TiAl- and Ni-based alloys with Zr-Al-NiCu bulk metallic glass. *Mater Des* 181 (2019) 107936.

Publisher's Note Springer Nature remains neutral with regard to jurisdictional claims in published maps and institutional affiliations.